

# 1 Repeated ice streaming on the northwest Greenland continental 2 shelf since the onset of the Middle Pleistocene Transition

3 Andrew M. W. Newton<sup>1,2</sup>, Mads Huuse<sup>1</sup>, Paul C. Knutz<sup>3</sup>, and David R. Cox<sup>1</sup>

4 <sup>1</sup>Department of Earth and Environmental Sciences, University of Manchester, Oxford Road, UK, M13 9PL.

5 <sup>2</sup>School of Natural and Built Environment, Queen's University Belfast, University Road, UK, BT7 1NN.

6 <sup>3</sup>Department of Geophysics, Geological Survey of Denmark and Greenland, Øster Voldgade 10, 1350,  
7 Copenhagen, Denmark.

8 *Correspondence to:* Andrew M. W. Newton (amwnewton@gmail.com)

9

10 **Abstract.** Ice streams provide a fundamental control on ice sheet discharge and depositional patterns along  
11 glaciated margins. This paper investigates ancient ice streams by presenting the first 3D seismic geomorphological  
12 analysis of a major glacial successions offshore Greenland. In Melville Bugt, northwest Greenland, six sets of  
13 landforms (five buried and one on the seafloor) have been interpreted as mega-scale glacial lineations (MSGL) that  
14 provide evidence for extensive ice streams on outer palaeo-shelves. A gradual change in mean MSGL orientation  
15 and associated depocentres through time suggests that the palaeo-ice flow and sediment transport pathways  
16 migrated in response to the evolving submarine topography through each glacial-interglacial cycle. The  
17 stratigraphy and available chronology show that the MSGL are confined to separate stratigraphic units and were  
18 most likely formed during several glacial stages since the onset of the Middle Pleistocene Transition at ~1.3 Ma.  
19 The MSGL record in Melville Bugt suggests that since ~1.3 Ma, ice streams regularly advanced across the  
20 continental shelf during glacial stages. High-resolution buried 3D landform records such as these have not been  
21 previously observed anywhere on the Greenland continental shelf margin and provide a crucial benchmark for  
22 testing how accurately numerical models are able to recreate past configurations of the Greenland Ice Sheet.

23

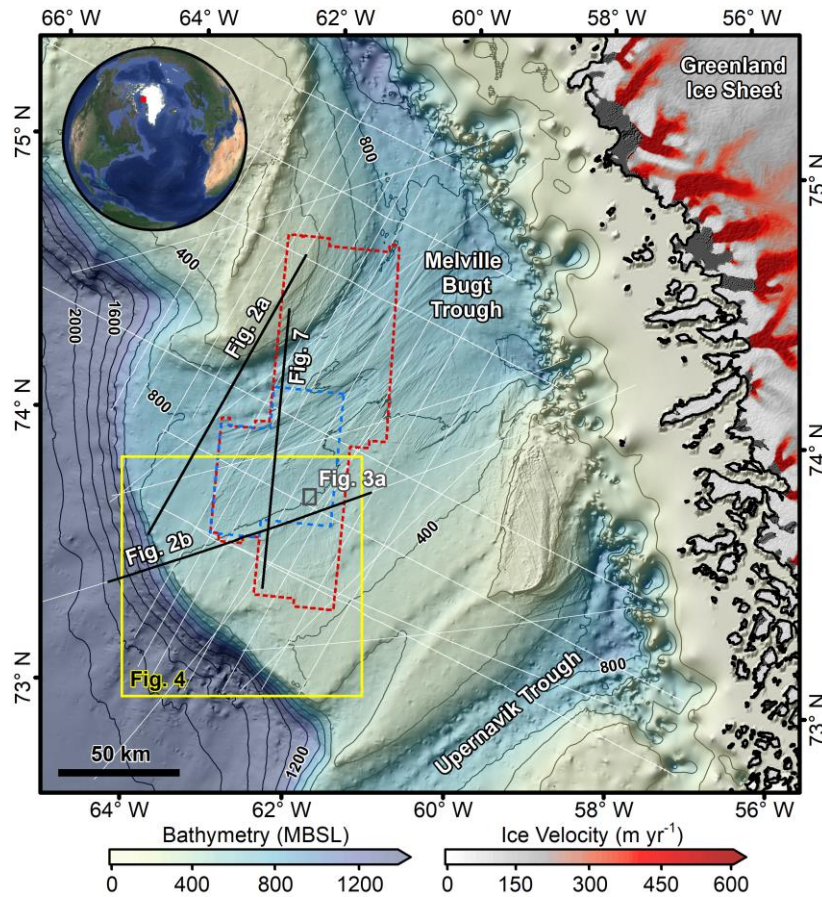
## 24 **1. Introduction**

25 The northwest sector of the Greenland Ice Sheet (GrIS) is currently experiencing some of the largest mass losses  
26 across the ice sheet (Mouginot et al., 2019). During the Pleistocene the northwest sector has also been shown to  
27 have experienced major changes in ice margin extent through multiple glacial-interglacial cycles (Knutz et al.,  
28 2019). To better project the future evolution of the northwest Greenland ice sheet, and the GrIS as a whole, requires  
29 the reconstruction of past configurations of the ice sheet, the role and evolution through time of its ice streams, and  
30 an understanding of how the antecedent and evolving topography impacted ice flow patterns during past glacial  
31 stages. Typically, reconstruction involves using fragmented geological records to constrain or test numerical ice  
32 sheet models that attempt to map spatiotemporal changes in ice sheet extent and the dominant processes as the  
33 climate evolves across multiple glacial-interglacial cycles (Solgaard et al., 2011; Tan et al., 2018). Improving and  
34 building upon that fragmented geological record is, therefore, of considerable importance for helping to improve  
35 and calibrate these models – i.e. if models can accurately reconstruct the past, then we can have more confidence  
36 in what they project for the future.

37 Although much of the past offshore extent of the GrIS and its retreat is poorly resolved (Funder et al., 2011;  
38 Vasskog et al., 2015), there are some areas, such as the Uummannaq and Disko Troughs in the west and the  
39 Kangerlussuaq, Westwind, and Norske Troughs in the east and northeast of Greenland, that have been surveyed.  
40 Geophysical data and shallow marine cores have been used to document landforms from the Last Glacial Maximum  
41 (LGM) on the continental shelf, deglacial ages, and retreat styles – with retreat often punctuated by Younger Dryas  
42 stillstands and an intricate relationship between calving margins and ocean currents (Arndt et al., 2017; Dowdeswell  
43 et al., 2010; Hogan et al., 2016; Jennings et al., 2014; Sheldon et al., 2016). Seismic reflection data have been used  
44 to explore evidence of older glaciations and show that the GrIS repeatedly advanced and retreated across the  
45 continental shelves of west and east Greenland through much of the late Pliocene and Pleistocene (Hofmann et al.,  
46 2016; Knutz et al., 2019; Laberg et al., 2007; Pérez et al., 2018). These seismic data show that GrIS extent has  
47 varied by 100s km throughout the Pleistocene and offers additional constraining observations to borehole and  
48 outcrop data that provide conflicting evidence that Greenland could have been nearly ice-free or persistently ice-  
49 covered for parts of the Pleistocene (Bierman et al., 2016; Schaefer et al., 2016).

50 To help understand long-term climatic changes, especially those associated with ice streams during glacial maxima,  
51 landforms observed on palaeo-seafloor surfaces mapped from 3D seismic data can provide information on past ice

52 sheet geometries and ice streaming locations. Landforms can be observed on surfaces preserved within trough-  
 53 mouth fans (TMFs), typically deposited on the middle and upper continental slope, or on palaeo-shelf layers buried  
 54 on the middle and outer continental shelf that built out as the TMF prograded (Ó Cofaigh et al., 2003). Here, for  
 55 the first time offshore Greenland, buried glacial landforms preserved on palaeo-shelves are documented using 3D  
 56 seismic reflection data from Melville Bugt (Fig. 1). Whilst ice streams are thought to have been present in Melville  
 57 Bugt since ~2.7 Ma (Knutz et al., 2019), these landforms provide new, direct, and detailed evidence of ice flow  
 58 pathways for six episodes of ice stream advance onto the outer continental shelf of Melville Bugt since ~1.3 Ma.



59

60 **Figure 1:** Seabed morphology and ice-flow velocity around the study area. The grey bathymetric contours are  
 61 every 200 m and the blue/red dashed lines show the outline of the 3D seismic surveys (blue is a high resolution  
 62 sub-crop of the original data that was reprocessed). The thin white lines show the locations of 2D seismic data.  
 63 Mean ice velocity from MEaSURES (cf. Joughin et al., 2010) shows contemporary outlet glaciers flowing into  
 64 northeastern Baffin Bay. Bathymetry combined from Jakobsson et al. (2012), Newton et al. (2017), and Knutz et  
 65 al. (2019). Locations of other figures shown. All figures plotted in UTM Zone 21N.

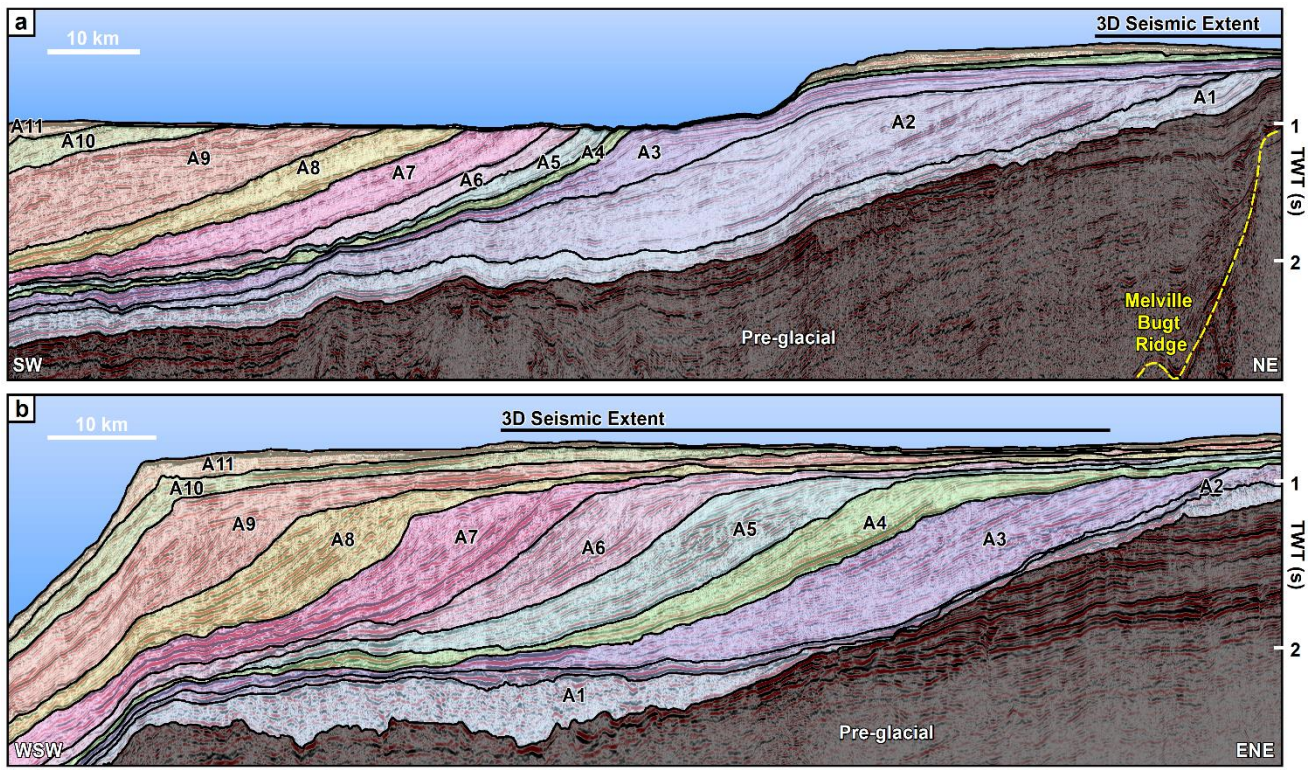
66

## 67 2. Background

68 Ice streams are corridors of fast-flowing ice that that can measure >20 km wide, 100s km long, with velocities  
69 >400-500 m yr<sup>-1</sup> (Bennett, 2003). Both in the present and in the geological past, ice streams have been important  
70 conduits for ice sheet mass redistribution and sediment delivery to ice sheet margins (Vorren and Laberg, 1997).  
71 Mega-scale glacial lineations (MSGSL) are elongated landforms (typically 1-10 km long) that form by the  
72 streamlining (Clark et al., 2003) or accretion of subglacial sediments (Spagnolo et al., 2016) beneath fast-flowing  
73 ice (Clark, 1993). This association is supported by observations of similar MSGSL features beneath the present-day  
74 Rutford Ice Stream in West Antarctica (King et al., 2009). MSGSL thought to date to the LGM have been observed  
75 on the present-day seafloor of the Melville Bugt study area (Fig. 1) and typically measure 4–6 km long, 100–200  
76 m wide, and 10–20 m high (Newton et al., 2017; Slabon et al., 2016). The MSGSL on the outermost continental  
77 shelf show that fast-flowing ice occupied the Melville Bugt Trough and reached the shelf edge, before retreating  
78 and experiencing changes in ice flow pathways, as is indicated by cross-cutting MSGSL on the middle continental  
79 shelf (Newton et al., 2017).

80 The glacial stratigraphy in Melville Bugt (Fig. 1) extends across an area of ~50,000 km<sup>2</sup> and measures up to ~2 km  
81 thick. The succession records advance and retreat of the northwest GrIS across the continental shelf multiple times  
82 since ~2.7 Ma and is subdivided into 11 major prograding units separated by regional unconformities (Knutz et al.,  
83 2019). The stratigraphy is partly age-constrained by a number of dates extracted from microfossil (~2.7 Ma) and  
84 palaeomagnetic data (~1.8 Ma) (Christ et al., 2020; Knutz et al., 2019). These dates suggest that whilst sediment  
85 accumulation likely varied over orbital and sub-orbital timescales, over periods longer than this (0.5-1.0 Myr) it  
86 did not change substantially and was grossly linear through time since glacigenic deposition began (Knutz et al.,  
87 2019). In the northern part of the trough topset preservation is limited due to more recent glacial erosion that has  
88 cut into the substrate (Fig. 2a), whereas in the south there is better preservation of aggradational topset strata (Fig.  
89 2b) – i.e. palaeo-shelves where buried landforms might be found.





90

91 **Figure 2:** Seismic cross-section profiles through the glacial successions. The fan comprises 11 seismic  
 92 stratigraphic units bounded by glacial unconformities formed since ~2.7 Ma (Knutz et al., 2019). The tentative  
 93 chronology from Knutz et al. (2019) suggests that the palaeo-seafloor surfaces preserved within units A7-A9 likely  
 94 cover a time period from ~1.3-0.43 Ma. This time period captures much of the Middle Pleistocene (781-126 ka)  
 95 and the transition into it from ~1.3 Ma. Locations of the lines are shown on Fig. 1. TWT is two-way-travel time.  
 96 Interpreted and uninterpreted seismic lines are provided as supplementary material.

97

### 98 3. Methods

99 This study used industry 3D and 2D seismic reflection data from Melville Bugt, northwest Greenland (Fig. 1). The  
 100 vertical resolution of the glacial successions is ~10-15 m and the horizontal resolution ~20-30 m – based on  
 101 frequencies ~30-50 Hz and a sound velocity ~2-2.2 km s<sup>-1</sup>. Horizons were picked from within the 3D seismic data  
 102 as part of a seismic geomorphological analysis (Posamentier, 2004), and gridded as 25x25 m two-way-time surface  
 103 maps – i.e. buried palaeo-seafloor maps. It is important to note that unlike traditional seafloor studies carried out  
 104 on bathymetric data, these palaeo-seafloor surfaces will have subsided and compacted since being buried. This  
 105 means that landform thicknesses likely represent a minimum estimate of their original morphology. Seismic  
 106 attributes, including variance and Root-Mean Square (RMS) amplitude, were extracted across the surfaces to aid

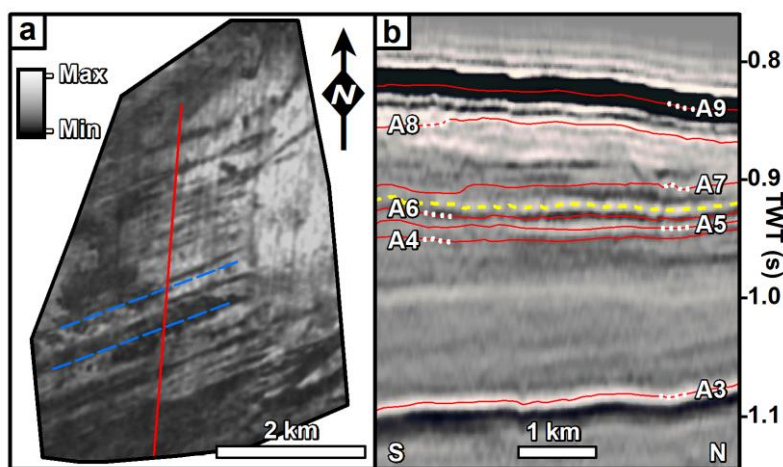
107 in visualising architectural elements and landforms. This study focused on identifying glacial landforms and used  
 108 published examples to guide interpretation (e.g. Dowdeswell et al., 2016). Where possible, using the velocity model  
 109 of Knutz et al. (2019), thickness maps were created for sub-units derived from deposits that were stratigraphically  
 110 linked to surfaces containing glacial landforms – e.g. correlative slope deposits onlapping the profile of the  
 111 glacially-influenced clinof orm reflection. These depocentre maps can be used to document where sediments have  
 112 been eroded and deposited, providing insight into how depositional patterns may have changed in response to the  
 113 evolution of ice streams pathways. In the absence of precise dating for each surface, the linear age model of Knutz  
 114 et al. (2019) has been used to relatively date glacial landforms identified in the different prograding units.

115

#### 116 4. Subglacial landforms

117 Seismic geomorphological analysis of topset strata imaged in the 3D data showed four sets of buried streamlined  
 118 features 5-15 km long and 200-300 m wide (Fig. 3 and 4). The landforms are typically 10-15 m high and although  
 119 they are close to vertical seismic resolution limits (meaning that cross-sectional profiles are subtle) they are best  
 120 observed in planform using the RMS amplitude or hillshaded surfaces. The streamlined features display a parallel  
 121 concordance, are confined to individual palaeo-shelf layers within separate stratigraphic units, and their trend cross-  
 122 cuts acquisition lines obliquely (Fig. 3 and 4). These features are interpreted as MSGL due to their morphology  
 123 (Spagnolo et al., 2014), and similarity to MSGL observed on the local seafloor (Newton et al., 2017) and buried on  
 124 other margins (e.g. Andreassen et al., 2007; Dowdeswell et al., 2006; Montelli et al., 2017; Rea et al., 2018).

125



126 **Figure 3:** (a) MSGL set 1, the oldest example of mega-scale glacial lineations (blue dashed lines) displayed as an  
 127 RMS image observed from 3D seismic reflection data and within unit A7 (b). The colour bar shows the maximum

128 and minimum RMS values. Note that this surface is only partially preserved due to subsequent glacial erosion. For  
129 location see Fig. 1. **(b)** Seismic cross-section profile showing the stratigraphic position (dashed yellow line) of the  
130 surface imaged in (a). The red lines show the top surface of each unit in the glacial successions and the dashed  
131 white lines are to help differentiate the labels to surfaces in this condensed stratigraphy. The location of the cross-  
132 section profile is shown by the red line on (a). Interpreted and uninterpreted seismic lines are provided as  
133 supplementary material.

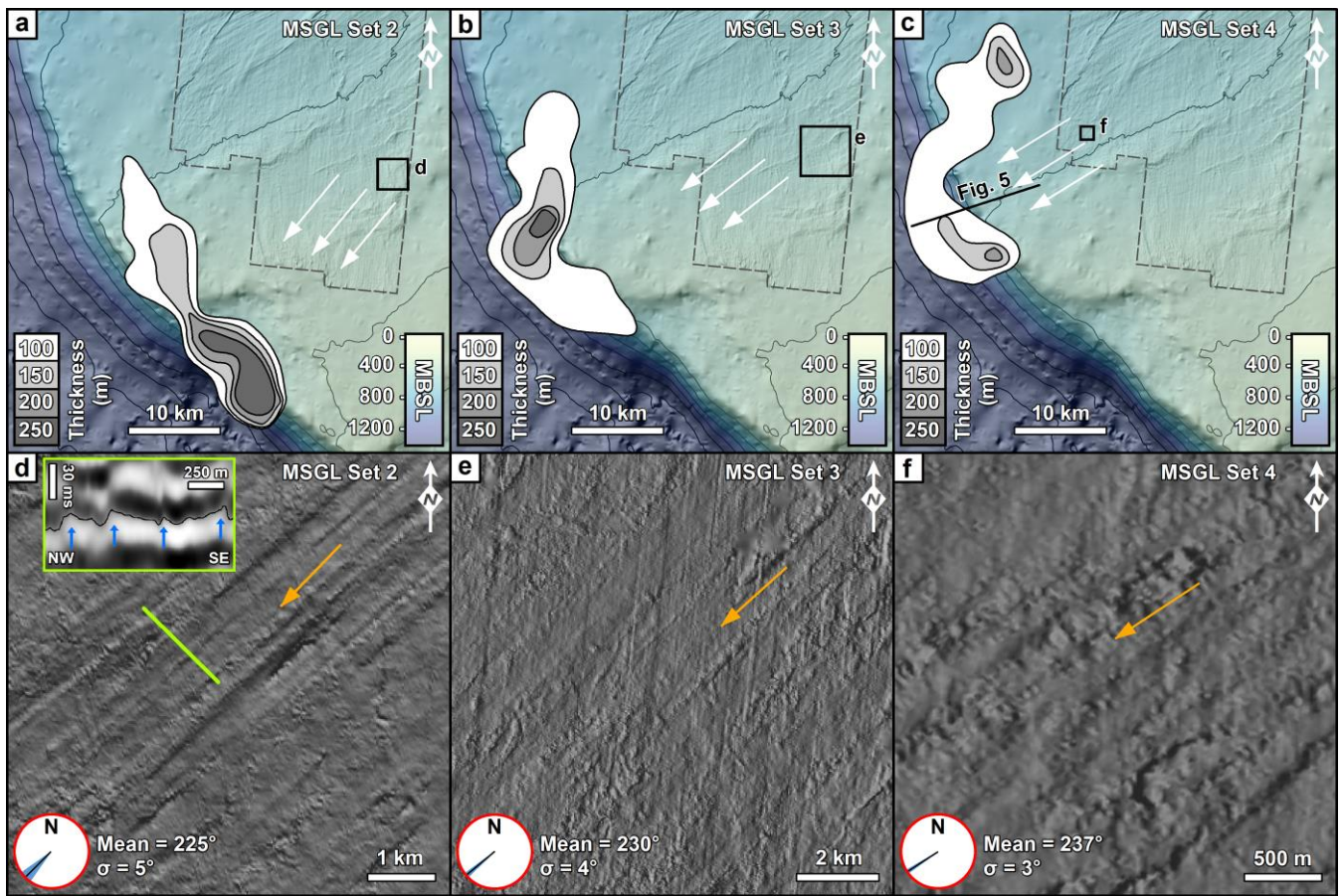
---

134

135 MSGL set 1 is the oldest and is observed with an orientation of  $254^\circ$  on a partially-preserved surface in the lowest  
136 part of a condensed section of unit A7 (~1.3-1.05 Ma) (Fig. 3). It was not possible to confidently determine  
137 correlative slope deposits and the associated depocentre due to the limited spatial extent of their preservation.  
138 Rising through the stratigraphy, MSGL set 2 is observed in the upper part of unit A8 (~1.05-0.65 Ma) (Fig. 4a) and  
139 the associated depocentre is located in the southwestern part of the study area and measures up to 250 m thick. All  
140 of the sub-unit depocentres show sediment thicknesses greater than 100 m and have been mapped from the slope  
141 deposits that are correlative to the adjacent palaeo-shelves. The slope deposits are typically comprised of onlapping  
142 chaotic seismic packages interpreted as stacked glacial debris (Fig. 5) (Vorren et al., 1989). MSGL set 2 has  
143 an average compass bearing of  $225^\circ$  ( $\sigma = 5^\circ$ ) that aligns well with the maximum depocentre thickness (Fig. 4a).  
144 MSGL sets 3 and 4 are observed on separate surfaces preserved within the topset strata of unit A9 (~0.65-0.45 Ma)  
145 (Fig. 4b, c, e, f,) and their bearings show a gradual transition to  $237^\circ$  from the  $225^\circ$  observed in unit A8 (Fig. 6).

146





147

148 **Figure 4:** Buried MSGL and associated TMF thickness maps. Panels (a) to (c) show the geographic location of  
 149 MSGL sets 2-4 displayed as hillshade images on panels (d) to (f). The dashed grey line on (a) to (c) is the 3D  
 150 seismic survey outline overlain on the contemporary seafloor, the white arrows show the inferred ice flow direction  
 151 from the MSGL, and the contoured outlines show the thickness of the sedimentary deposit associated with MSGL  
 152 sets 2-4. Orange arrows on panels (d) to (f) show the inferred ice flow direction. On panel (d) the green line displays  
 153 the location of the inset cross-section profile of the MSGL. Blue arrows point to the mounded features visible on  
 154 the hillshade image. The red circles in (d) to (f) display average MSGL compass bearings (black line) and the  
 155 standard deviation (blue fan beneath) for each panel. Location of panels (a) to (c) shown on Fig. 1. The relative  
 156 ages and stratigraphic positions of each MSGL set are discussed in the text and labelled on Fig. 6.

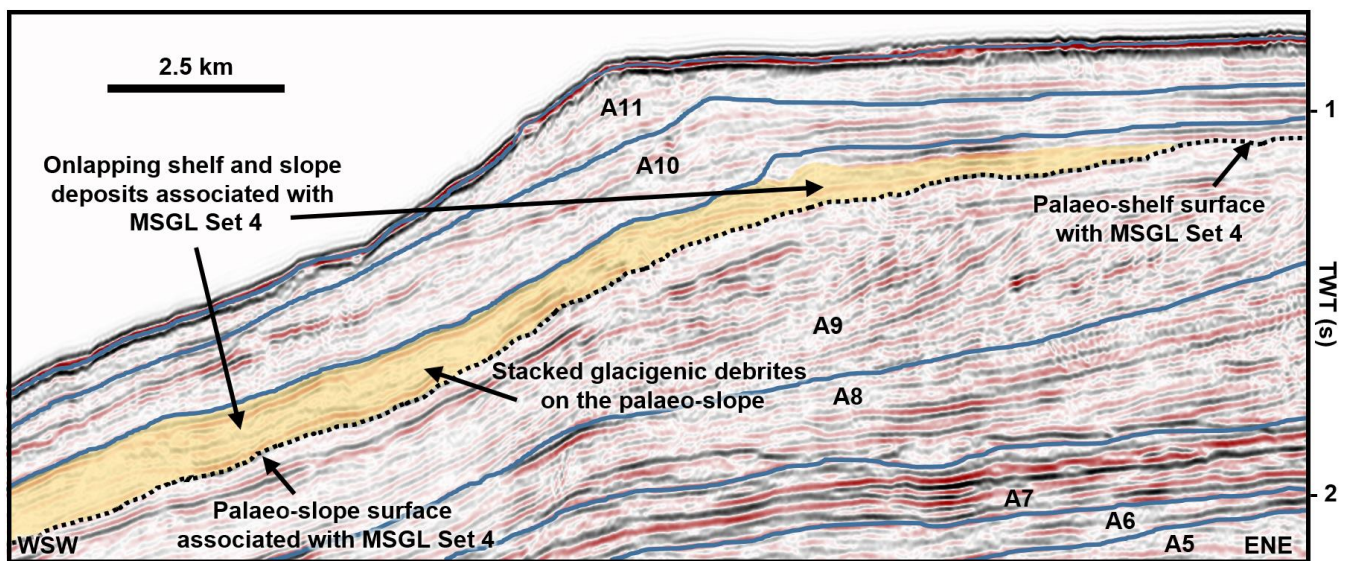
157

158 Although the 3D seismic data do not cover the distal part of the succession, by using examples of MSGL that have  
 159 been observed in 3D (Fig. 3, 4), the 2D seismic data were investigated for similar cross-sectional features. In unit  
 160 A10 (~0.45-0.35 Ma) a reflection on the outer continental shelf shows a similar corrugated morphology, with  
 161 heights of 10-15 m and widths of 200-300 m, to the MSGL pattern observed in the 3D data (Fig. 6b). The MSGL



162 documented in the 3D data also show that ice previously flowed towards this general area (Fig. 6c). The  
163 interpretation as MSGL set 5 is less robust due to the lack of 3D data and whilst it is not possible to unequivocally  
164 rule out that these features are something else, such as iceberg scours, an interpretation of MSGL is supported by  
165 the location of these features in topset strata above the glacial unconformity that marks the top of unit A9,  
166 suggesting the presence of grounded and erosive ice on the outer continental shelf, conditions generally associated  
167 with MSGL formation.

168 The final set of MSGL (set 6) is observed in unit A11 (~0.35-0 Ma) on the seafloor and has been interpreted as a  
169 grounded ice stream on the outer continental shelf at the LGM by Newton et al. (2017) (Fig. 6c). These MSGL  
170 show cross-cutting evidence that allow for changes in ice flow patterns to be deduced. The oldest MSGL on the  
171 seafloor suggest an ice flow towards the west-southwest that is parallel to the axis of the trough, whilst the younger  
172 MSGL (i.e. those which cross-cut the older MSGL) show an ice flow toward the south-southwest, suggesting a  
173 change in ice flow during deglaciation (Newton et al., 2017).



174  
175 **Figure 5:** Seismic cross-section profile showing the main glaciogenic units and the palaeo-shelf surface (dotted line)  
176 where MSGL set 4 is observed. Onlapping and stacked debrite packages are interpreted to be genetically linked to  
177 deposition caused by the ice stream that formed this set of MSGL and are used as an indicator of the broad  
178 depositional patterns displayed in Fig. 4c. Line location is shown on Fig. 4c. Interpreted and uninterpreted seismic  
179 lines are provided as supplementary material.

180

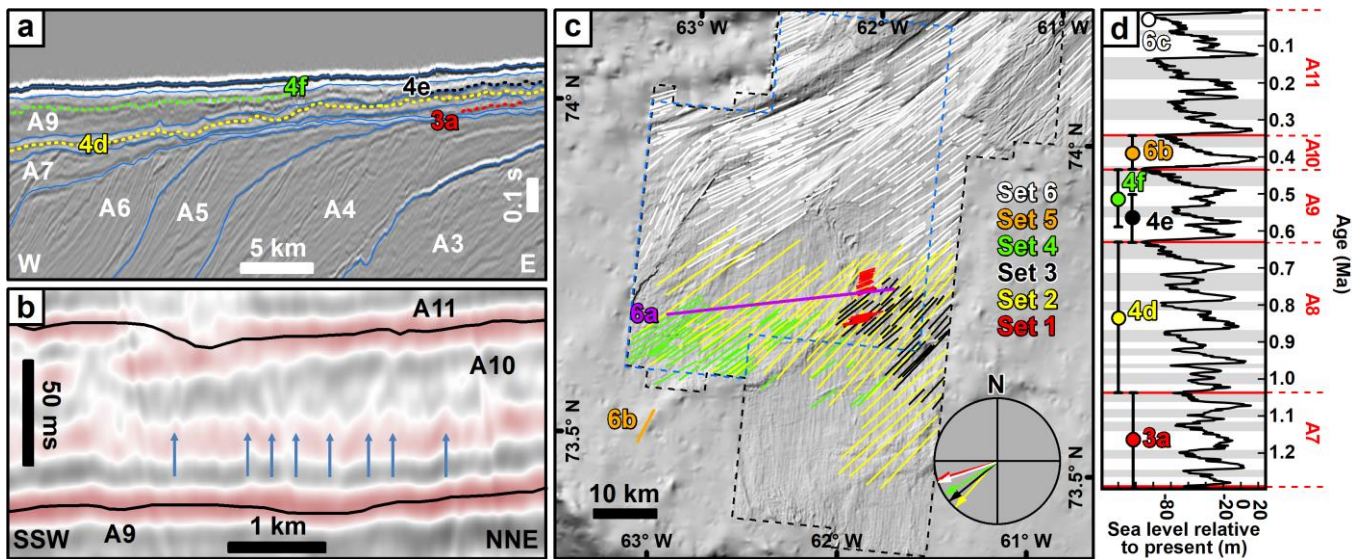
## 181 5. Palaeo-ice streams

182 The previous lack of 3D seismic data coverage means that ice stream landforms have not been observed for glacials  
183 preceding the LGM on the Greenland margin. Information on past ice flow patterns has, therefore, relied upon  
184 broad inferences from depocentre locations – i.e. areas where large volumes of sediment are associated with the  
185 general pathway of ice streams. Using the new seismic, six sets of ice stream landforms have been documented –  
186 one on the seafloor, four buried surfaces imaged in 3D, and one captured in the 2D seismic. The MSGL sets provide  
187 evidence for multiple ice streaming events on the northwest Greenland continental shelf prior to, and including, the  
188 LGM. Limited chronological constraints are currently available to determine exact timings, but the available  
189 chronology suggests these features formed during six glacial stages after ~1.3 Ma (Knutz et al., 2019). Although  
190 no older MSGL have been imaged on palaeo-shelves captured in the available 3D seismic data, ice streams are  
191 inferred to have operated in the area prior to ~1.3 Ma, based on the large volumes of sediment delivered to the  
192 margin (Knutz et al., 2019). It is noteworthy that the first observations of MSGL occur at the onset of a major  
193 change in the depositional patterns of the Melville Bugt and Upernavik TMFs. Unit A7 was deposited when the  
194 Melville Bugt and Upernavik TMFs combined to form an elongate depocentre up to 1 km thick. During the  
195 subsequent deposition of unit A8 the TMFs separated into discrete depocentres up to 700 m thick, signalling a  
196 possible reorganisation in ice flow in the region (Knutz et al., 2019). The reasons for this change are unresolved,  
197 but modification of the submarine topography brought about by glacigenic deposition and erosion, such as  
198 presented here, may have forced adjustments in the ice sheet flow on the outer continental shelf due to changes in  
199 available accommodation.

200 Switches in ice stream pathways on continental shelves between different glacial maxima have been observed on  
201 the mid-Norwegian margin, where new cross-shelf troughs were formed through the erosive action of ice  
202 (Dowdeswell et al., 2006). In contrast to the mid-Norwegian margin, the available data in Melville Bugt does not  
203 show evidence of buried cross-shelf troughs. The observations show changes in ice stream pathways that appear to  
204 have occurred more gradually between each MSGL set but remained focused within the confines of the pre-existing  
205 trough. The longevity of the Northern Bank and the significant overdeepening of the inner trough (cf. Newton et  
206 al., 2017) likely provided consistent topographic steering of ice streams on the inner continental shelf. On the outer  
207 continental shelf, deposition during the preceding glacial stage likely forced gradual ice stream migration northward  
208 due to this deposition reducing the available accommodation for subsequent glacial stages (Fig. 7). Thickness maps  
209 associated with MSGL sets 2-4 demonstrate this gradual, rather than extreme, shift in ice stream drainage pathways

210 that is supported by 5-6° shifts in the mean orientation of each MSGL set from 225° during unit A8 time, to 237°  
211 during unit A9 (Fig. 4). This shift continued at the LGM where the majority of MSGL on the outer continental  
212 shelf – except for some cross-cutting related to deglaciation (Newton et al., 2017) – show a mean orientation of  
213 ~248° (Fig. 6c).

214 The partial preservation of the different palaeo-shelves means ice margin fanning on the less topographically-  
215 confined outer continental shelf cannot be definitively ruled out as an explanation for differing MSGL orientations.  
216 However, the observed metrics and depocentre migration provide complementary evidence that this was in  
217 response to a gradual migration of the main ice stream flow pathway – i.e. ice flow pathways gradually moved  
218 northward in a clockwise pattern from unit A8 onwards (~1 Ma). The gradual shift northward of the main ice stream  
219 pathway and its associated erosion meant that topset deposits in the south, with each passing glacial stage, were  
220 increasingly less impacted by the ice stream erosion and therefore the landforms that they contained had a better  
221 chance of being preserved through subsequent glacial stages. The Melville Bugt Trough is the widest in Greenland  
222 (Newton et al., 2017) and it is possible that the preservation of these topsets is a consequence of this. The  
223 preservation suggests that whilst the main palaeo-ice stream trunks associated with each glacial stage were  
224 accommodated within the broad confines of the trough, the fast-flowing and most erosive ice did not occupy its  
225 full width – e.g. there are no MSGL present for the LGM (set 6) in the southern part of the trough. The northward  
226 migration of the main ice stream pathway is also reflected by erosion and cutting into the deposits of the Northern  
227 Bank (Fig. 7). Although ice stream margin fanning or changes in upstream ice sheet controls cannot be ruled out,  
228 the gradual depocentre and MSGL migration suggests that deposition during successive glacial stages may have  
229 been sufficient to bring about small changes in flow directions and subsequent depositional patterns. Future ice  
230 sheet modelling can contribute to this discussion by exploring whether ice volume over northern Greenland would  
231 have been sufficient to maintain ice flux if the ice streams occupied the full width of the Melville Bugt Trough. To  
232 a lesser extent, it is possible that the Melville Bugt Ridge, an underlying tectonic structure which has previously  
233 generated accommodation in the southern part of the basin through differential subsidence (Cox et al., 2020; Knutz  
234 et al., 2019), could have contributed to reducing potential erosion of aggradational topsets by increasing palaeo-  
235 water depths to the point where ice grounding was significantly reduced or removed.



236

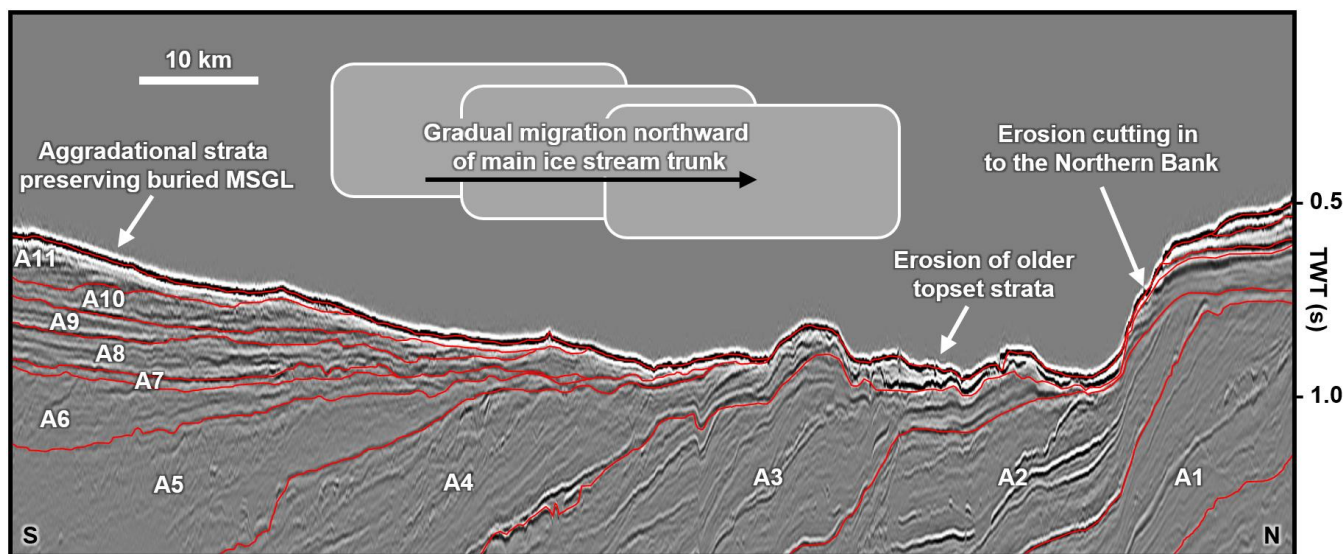
237 **Figure 6:** (a) Seismic cross-section profile showing the stratigraphic location of the surfaces shown in Fig. 3 and  
 238 4. The blue lines are the tops of the units shown on Fig. 2. The location of the line is shown on Fig. 6c. (b) Seismic  
 239 cross-section profile from 2D seismic survey showing evidence for potential MSGL (blue arrows) in unit A10 on  
 240 the outer continental shelf. Seismic line location is shown on Fig. 6c. (c) Digitized MSGL record from 3D seismic  
 241 data. Set 6 represents the LGM record from Newton et al. (2017) and sets 1-5 from the current study. The compass  
 242 shows the mean bearings for each set of MSGL with the exception of set 5 because it is not captured in 3D. (d)  
 243 Possible age range for each MSGL surfaces observed within the glacial units of Knutz et al. (2019) and  
 244 compared against the global sea level record (Miller et al., 2011). Grey bands are glacial stages. Note that in all the  
 245 panels, the surfaces (a), digitised MSGL (c), mean flow bearings (c), and labels (d) are colour-coded to ease cross-  
 246 referencing. Interpreted and uninterpreted seismic lines are provided as supplementary material.

247

248 In the wider context of the whole GrIS, in east Greenland, sedimentological and geophysical evidence suggest that  
 249 early in the Middle Pleistocene Transition (MPT - ~1.3 Ma to 0.7 Ma) ice advanced across the continental shelf  
 250 (Laberg et al., 2018; Pérez et al., 2019), whilst offshore southern Greenland documentation of increased ice-rafted  
 251 detritus suggests a similar ice advance (St. John and Krissek, 2002). MPT ice sheet expansions have been  
 252 documented in the Barents Sea (Mattingsdal et al., 2014), on the mid-Norwegian margin (Newton and Huuse,  
 253 2017), the North Sea (Rea et al., 2018), and in North America (Balco and Rovey, 2010), highlighting a response of  
 254 all major Northern Hemisphere ice sheets to a currently unresolved climate forcing. Although ice streaming in  
 255 Melville Bugt continued after the MPT and through to the latest Pleistocene, some studies from lower latitude areas



256 of west and east Greenland show reduced ice stream erosion and deposition at this time (Hofmann et al., 2016;  
257 Pérez et al., 2018), perhaps suggesting the high latitude locality of Melville Bugt or the overdeepened and  
258 bottlenecked geometry (topographic constraints) of the inner trough (Newton et al., 2017) helped promote  
259 conditions favourable for ice streaming.



260

261 **Figure 7:** Interpreted seismic strike cross-section profile across the continental shelf showing spatially variable  
262 preservation of topset deposits associated with the main depositional units. This variable preservation is thought to  
263 relate to the gradual migration of the ice stream away from the areas of higher topography that contain the  
264 aggradational strata. This northward migration of the ice stream pathways is also reflected by the erosion of the  
265 southern flank of the Northern Bank. Location of the line is shown on Fig. 1. Interpreted and uninterpreted seismic  
266 lines are provided as supplementary material.

267

268 The MSGL record presented here provides some additional insight into the contradictory records on the longevity  
269 of the GrIS. Schaefer et al. (2016) showed that cosmogenic signatures require ice-free periods during the  
270 Pleistocene and whilst these ice-free periods need not have occurred since 1.1 Ma, ice sheet loss could have  
271 occurred during or after the MPT. Ice stream evolution has been shown to have led to rapid ice sheet changes on  
272 other ancient ice sheets (Sejrup et al., 2016), and given that ~16% of the GrIS currently drains into Melville Bugt  
273 (Rignot and Mouginot, 2012) the ice streams documented here could have contributed to major changes in ice sheet  
274 organisation and extent – indeed, the numerical model used by Schaefer et al. (2016) requires the early loss of the  
275 northwest GrIS during ice sheet collapse. Fully resolving issues like this requires numerical ice sheet models that

276 are capable of reproducing fragmented geological evidence. For example, recent modelling exploring Pleistocene  
277 climate evolution (Willeit et al., 2019) provides palaeo-geographic maps of ice sheet extent that do not capture the  
278 ice sheet extent inferred from buried landform records on many glaciated margins (e.g. Rea et al., 2018), including  
279 Melville Bugt. Thus, there is currently a mismatch between modelling outputs and landform records. If these  
280 models are not able to recreate ice sheet extent, ice stream locations, and flow pathways that have been extracted  
281 from the geological record then those models will require refinement before they can be used as a tool for projecting  
282 future GrIS evolution. These potential discrepancies underline how geological records, such as those presented  
283 here, provide crucial empirical constraints for modelling the GrIS across multiple glacial-interglacial cycles.

284

## 285 **6. Conclusions**

286 This study provides a seismic geomorphological analysis offshore northwest Greenland and documents, for the  
287 first time, several sets of buried MSGL on the Greenland margin. The observation of different MSGL sets in  
288 separate stratigraphic layers confirms the presence of fast-flowing ice streams during at least six glacial maxima  
289 since the onset of the Middle Pleistocene Transition at ~1.3 Ma. These landform records show that grounded and  
290 fast-flowing ice advanced across the continental shelf to the palaeo-shelf edge of northwest Greenland, with each  
291 subsequent ice stream flow pathway being partly controlled by the deposits left behind by the ice streams that  
292 preceded it. This represents a first spatio-temporal insight into sediment deposition and ice flow dynamics of  
293 individual ice streams during glacial maxima since ~1.3 Ma in Melville Bugt. These results help to further  
294 emphasise why northwest Greenland would be suitable for future ocean drilling that will help to elucidate ice sheet  
295 and climate history of the region.

296

## 297 **Data availability**

298 The Geological Survey of Denmark and Greenland or the authors should be contacted to discuss access to the raw  
299 seismic reflection data.

300

## 301 **Author contribution**

302 AMWN carried out the seismic geomorphological study, drafted the figures, and wrote the initial text. All other  
303 authors contributed to interpretation and manuscript preparation.

304

### 305 **Competing interests**

306 There are no competing interests to declare.

307

### 308 **Acknowledgements**

309 AMWN was supported by the Natural Environment Research Council (NERC - NE/K500859/1) and Cairn Energy.  
310 DRC was funded by NERC and the British Geological Survey (NE/M00578X/1). Schlumberger and ESRI are  
311 thanked for Petrel and ArcGIS software. All authors thank Cairn Energy and Shell for data and permission to  
312 publish. Simon H. Brocklehurst is thanked for pre-reviewing this work and offering valuable insights. Brice R.  
313 Rea, Lara F. Perez, an anonymous reviewer, and the editor are thanked for helpful comments and handling of the  
314 manuscript.

315

### 316 **References**

317 Andreassen, K., Ødegaard, C. M. and Rafaelsen, B.: Imprints of former ice streams, imaged and interpreted using  
318 industry three-dimensional seismic data from the south-western Barents Sea, in *Seismic geomorphology:  
319 applications to hydrocarbon exploration and production*, edited by R. J. Davies, H. W. Posamentier, L. W. Wood,  
320 and J. A. Cartwright, pp. 151–169, Geological Society Special Publication., 2007.

321 Arndt, J. E., Jokat, W. and Dorschel, B.: The last glaciation and deglaciation of the Northeast Greenland  
322 continental shelf revealed by hydro-acoustic data, *Quat. Sci. Rev.*, 160, 45–56,  
323 doi:10.1016/j.quascirev.2017.01.018, 2017.

324 Balco, G. and Rovey, C. W.: Absolute chronology for major Pleistocene advances of the Laurentide ice Sheet,  
325 *Geology*, 38, 795–798, doi:10.1130/G30946.1, 2010.

326 Bennett, M. R.: Ice streams as the arteries of an ice sheet: Their mechanics, stability and significance, *Earth-*  
327 *Science Rev.*, 61, 309–339, doi:10.1016/S0012-8252(02)00130-7, 2003.

328 Bierman, P. R., Shakun, J. D., Corbett, L. B., Zimmerman, S. R. and Rood, D. H.: A persistent and dynamic East  
329 Greenland Ice Sheet over the past 7.5 million years, *Nature*, 540, 256–260, doi:10.1038/nature20147, 2016.

330 Christ, A. J., Bierman, P. R., Knutz, P. C., Corbett, L. B., Fosdick, J. C., Thomas, E. K., Cowling, O. C., Hidy, A.  
331 J. and Caffee, M. W.: The Northwestern Greenland Ice Sheet During The Early Pleistocene Was Similar To  
332 Today, *Geophys. Res. Lett.*, 47(1), doi:10.1029/2019GL085176, 2020.

333 Clark, C. D.: Mega-scale glacial lineations and cross-cutting ice-flow landforms, *Earth Surf. Process. Landforms*,  
334 18, 1–29, doi:10.1002/esp.3290180102, 1993.

335 Clark, C. D., Tulaczyk, S. M., Stokes, C. R. and Canals, M.: A groove-ploughing theory for the production of  
336 mega-scale glacial lineations, and implications for ice-stream mechanics, *J. Glaciol.*, 49, 240–256,  
337 doi:10.3189/172756503781830719, 2003.

338 Cox, D. R., Huuse, M., Newton, A. M. W., Gannon, P. and Clayburn, J. A. P.: Slip Sliding Away: Enigma of  
339 Large Sandy Blocks within a Gas Bearing Mass Transport Deposit, Offshore NW Greenland, *Am. Assoc. Pet.*  
340 *Geol. Bull.*, 104(5), 1011–1044, doi:10.1306/10031919011, 2020.

341 Dowdeswell, J. A., Ottesen, D. and Rise, L.: Flow switching and large-scale deposition by ice streams draining  
342 former ice sheets, *Geology*, 34, 313–316, doi:10.1130/G22253.1, 2006.

343 Dowdeswell, J. A., Ottesen, D. and Rise, L.: Rates of sediment delivery from the Fennoscandian Ice Sheet  
344 through an ice age, *Geology*, 38, 3–6, doi:10.1130/G25523.1, 2010.

345 Dowdeswell, J. A., Canals, M., Jakobsson, M., Todd, B. J., Dowdeswell, E. K. and Hogan, K. A.: Atlas of  
346 Submarine Glacial landforms: Modern, Quaternary and Ancient, Geological Society of London., 2016.

347 Funder, S., Kjeldsen, K. K., Kjær, K. H. and O Cofaigh, C.: The Greenland Ice Sheet During the Past 300,000  
348 Years: A Review, in *Developments in Quaternary Science*, edited by J. Ehlers, P. L. Gibbard, and P. D. Hughes,  
349 pp. 699–713, Elsevier, Amsterdam., 2011.

350 Hofmann, J. C., Knutz, P. C., Nielsen, T. and Kuijpers, A.: Seismic architecture and evolution of the Disko Bay



351 trough-mouth fan, central West Greenland margin, *Quat. Sci. Rev.*, 147, 69–90,  
352 doi:10.1016/j.quascirev.2016.05.019, 2016.

353 Hogan, K. A., Ó Cofaigh, C., Jennings, A. E., Dowdeswell, J. A. and Hiemstra, J. F.: Deglaciation of a major  
354 palaeo-ice stream in Disko Trough, West Greenland, *Quat. Sci. Rev.*, 147, 5–26,  
355 doi:10.1016/j.quascirev.2016.01.018, 2016.

356 Jakobsson, M., Mayer, L., Coakley, B., Dowdeswell, J. A., Forbes, S., Fridman, B., Hodnesdal, H., Noormets, R.,  
357 Pedersen, R., Rebecco, M., Schenke, H. W., Zarayskaya, Y., Accettella, D., Armstrong, A., Anderson, R. M.,  
358 Bienhoff, P., Camerlenghi, A., Church, I., Edwards, M., Gardner, J. V., Hall, J. K., Hell, B., Hestvik, O.,  
359 Kristoffersen, Y., Marcussen, C., Mohammad, R., Mosher, D., Nghiem, S. V., Pedrosa, M. T., Travaglini, P. G.  
360 and Weatherall, P.: The International Bathymetric Chart of the Arctic Ocean (IBCAO) Version 3.0, *Geophys.*  
361 *Res. Lett.*, 39, L12609, doi:10.1029/2012GL052219, 2012.

362 Jennings, A. E., Walton, M. E., Ó Cofaigh, C., Kilfeather, A., Andrews, J. T., Ortiz, J. D., De Vernal, A. and  
363 Dowdeswell, J. A.: Paleoenvironments during Younger Dryas-Early Holocene retreat of the Greenland Ice Sheet  
364 from outer Disko Trough, central west Greenland, *J. Quat. Sci.*, 29, 27–40, doi:10.1002/jqs.2652, 2014.

365 St. John, K. E. K. and Krissek, L. A.: The late Miocene to Pleistocene ice-rafting history of Southeast Greenland,  
366 *Boreas*, 31, 28–35, doi:10.1111/j.1502-3885.2002.tb01053.x, 2002.

367 Joughin, I., Smith, B. E., Howat, I. M., Scambos, T. and Moon, T.: Greenland flow variability from ice-sheet-  
368 wide velocity mapping, *J. Glaciol.*, 56, 415–430, doi:10.3189/002214310792447734, 2010.

369 King, E. C., Hindmarsh, R. C. A. and Stokes, C. R.: Formation of mega-scale glacial lineations observed beneath  
370 a West Antarctic ice stream, *Nat. Geosci.*, 2(8), 585–588, doi:10.1038/ngeo581, 2009.

371 Knutz, P. C., Newton, A. M. W., Hopper, J. R., Huuse, M., Gregersen, U., Sheldon, E. and Dybkjær, K.: Eleven  
372 phases of Greenland Ice Sheet shelf-edge advance over the past 2.7 million years, *Nat. Geosci.*, 2019.

373 Laberg, J. S., Guidard, S., Mienert, J., Vorren, T. O., Haflidason, H. and Nygård, A.: Morphology and  
374 morphogenesis of a high-latitude canyon; the Andøya Canyon, Norwegian Sea, *Mar. Geol.*, 246, 68–85,  
375 doi:10.1016/j.margeo.2007.01.009, 2007.

376 Laberg, J. S., Rydningen, T. A., Forwick, M. and Husum, K.: Depositional processes on the distal Scoresby  
377 Trough Mouth Fan (ODP Site 987): Implications for the Pleistocene evolution of the Scoresby Sund Sector of the  
378 Greenland Ice Sheet, *Mar. Geol.*, 402, 51–59, doi:10.1016/j.margeo.2017.11.018, 2018.

379 Mattingsdal, R., Knies, J., Andreassen, K., Fabian, K., Husum, K., Grøsfjeld, K. and De Schepper, S.: A new  
380 6Myr stratigraphic framework for the Atlantic-Arctic Gateway, *Quat. Sci. Rev.*, 92, 170–178,  
381 doi:10.1016/j.quascirev.2013.08.022, 2014.

382 Montelli, A., Dowdeswell, J. A., Ottesen, D. and Johansen, S. E.: Ice-sheet dynamics through the Quaternary on  
383 the mid-Norwegian continental margin inferred from 3D seismic data, *Mar. Pet. Geol.*, 80, 228–242,  
384 doi:10.1016/j.marpetgeo.2016.12.002, 2017.

385 Mougnot, J., Rignot, E., Bjørk, A. A., van den Broeke, M., Millan, R., Morlighem, M., Noël, B., Scheuchl, B.  
386 and Wood, M.: Forty-six years of Greenland Ice Sheet mass balance from 1972 to 2018, *Proc. Natl. Acad. Sci.*,  
387 doi:10.1073/pnas.1904242116, 2019.

388 Newton, A. M. W. and Huuse, M.: Late Cenozoic environmental changes along the Norwegian margin, *Mar.*  
389 *Geol.*, 393, 216–244, doi:10.1016/j.margeo.2017.05.004, 2017.

390 Newton, A. M. W., Knutz, P. C., Huuse, M., Gannon, P., Brocklehurst, S. H., Clausen, O. R. and Gong, Y.: Ice  
391 stream reorganization and glacial retreat on the northwest Greenland shelf, *Geophys. Res. Lett.*, 44(15), 7826–  
392 7835, doi:10.1002/2017GL073690, 2017.

393 Ó Cofaigh, C., Taylor, J., Dowdeswell, J. A. and Pudsey, C. J.: Palaeo-ice streams, trough mouth fans and high-  
394 latitude continental slope sedimentation, *Boreas*, 32, 37–55, doi:10.1080/03009480310001858, 2003.

395 Pérez, L. F., Nielsen, T., Knutz, P. C., Kuijpers, A. and Damm, V.: Large-scale evolution of the central-east  
396 Greenland margin: New insights to the North Atlantic glaciation history, *Glob. Planet. Change*, 163, 141–157,  
397 doi:10.1016/j.gloplacha.2017.12.010, 2018.

398 Pérez, L. F., Nielsen, T., Rasmussen, T. L. and Winsborrow, M.: Quaternary interaction of cryospheric and  
399 oceanographic processes along the central-east Greenland margin, *Boreas*, 48, 72–91, doi:10.1111/bor.12340,  
400 2019.

401 Posamentier, H. W.: Seismic Geomorphology: Imaging Elements of Depositional Systems from Shelf to Deep  
402 Basin Using 3D Seismic Data: Implications for Exploration and Development, in 3D Seismic Technology:  
403 Application to the Exploration of Sedimentary Basins, edited by R. J. Davies, J. A. Cartwright, S. A. Stewart, M.  
404 Lappin, and J. R. Underhill, pp. 11–24, Geological Society of London., 2004.

405 Rea, B. R., Newton, A. M. W., Lamb, R. M., Harding, R., Bigg, G. R., Rose, P., Spagnolo, M., Huuse, M., Cater,  
406 J. M. L., Archer, S., Buckley, F., Halliyeva, M., Huuse, J., Cornwell, D. G., Brocklehurst, S. H. and Howell, J.  
407 A.: Extensive marine-terminating ice sheets in Europe from 2.5 million years ago, *Sci. Adv.*, 4(6),  
408 doi:10.1126/sciadv.aar8327, 2018.

409 Rignot, E. and Mouginot, J.: Ice flow in Greenland for the International Polar Year 2008-2009, *Geophys. Res.*  
410 *Lett.*, 39, L11501, doi:10.1029/2012GL051634, 2012.

411 Schaefer, J. M., Finkel, R. C., Balco, G., Alley, R. B., Caffee, M. W., Briner, J. P., Young, N. E., Gow, A. J. and  
412 Schwartz, R.: Greenland was nearly ice-free for extended periods during the Pleistocene, *Nature*, 540, 252–255,  
413 doi:10.1038/nature20146, 2016.

414 Sejrup, H. P., Clark, C. D. and Hjelstuen, B. O.: Rapid ice sheet retreat triggered by ice stream debuitressing:  
415 Evidence from the North Sea, *Geology*, 44, 355–358, doi:10.1130/G37652.1, 2016.

416 Sheldon, C., Jennings, A., Andrews, J. T., Ó Cofaigh, C., Hogan, K., Dowdeswell, J. A. and Seidenkrantz, M. S.:  
417 Ice stream retreat following the LGM and onset of the west Greenland current in Uummannaq Trough, west  
418 Greenland, *Quat. Sci. Rev.*, 147, 27–46, doi:10.1016/j.quascirev.2016.01.019, 2016.

419 Slabon, P., Dorschel, B., Jokat, W., Myklebust, R., Hebbeln, D. and Gebhardt, C.: Greenland ice sheet retreat  
420 history in the northeast Baffin Bay based on high-resolution bathymetry, *Quat. Sci. Rev.*, 154, 182–198,  
421 doi:10.1016/j.quascirev.2016.10.022, 2016.

422 Solgaard, A. M., Reeh, N., Japsen, P. and Nielsen, T.: Snapshots of the Greenland ice sheet configuration in the  
423 Pliocene to early Pleistocene, *J. Glaciol.*, 57(205), 871–880, doi:10.3189/002214311798043816, 2011.

424 Spagnolo, M., Clark, C. D., Ely, J. C., Stokes, C. R., Anderson, J. B., Andreassen, K., Graham, A. G. C. and  
425 King, E. C.: Size, shape and spatial arrangement of mega-scale glacial lineations from a large and diverse dataset,  
426 *Earth Surf. Process. Landforms*, 39(11), 1432–1448, doi:10.1002/esp.3532, 2014.

427 Spagnolo, M., Phillips, E., Piotrowski, J. A., Rea, B. R., Clark, C. D., Stokes, C. R., Carr, S. J., Ely, J. C.,  
428 Ribolini, A., Wysota, W. and Szuman, I.: Ice stream motion facilitated by a shallow-deforming and accreting bed,  
429 *Nat. Commun.*, 7, 10723, doi:10.1038/ncomms10723, 2016.

430 Tan, N., Ladant, J. B., Ramstein, G., Dumas, C., Bachem, P. and Jansen, E.: Dynamic Greenland ice sheet driven  
431 by pCO<sub>2</sub> variations across the Pliocene Pleistocene transition, *Nat. Commun.*, 9, 4755, doi:10.1038/s41467-018-  
432 07206-w, 2018.

433 Vasskog, K., Langebroek, P. M., Andrews, J. T., Nilsen, J. E. Ø. and Nesje, A.: The Greenland Ice Sheet during  
434 the last glacial cycle: Current ice loss and contribution to sea-level rise from a palaeoclimatic perspective, *Earth-*  
435 *Science Rev.*, 150, 45–67, doi:10.1016/j.earscirev.2015.07.006, 2015.

436 Vorren, T. O. and Laberg, J. S.: Trough mouth fans - Palaeoclimate and ice-sheet monitors, *Quat. Sci. Rev.*, 16,  
437 865–881, doi:10.1016/S0277-3791(97)00003-6, 1997.

438 Vorren, T. O., Lebesbye, E., Andreassen, K. and Larsen, K. B.: Glacigenic sediments on a passive continental  
439 margin as exemplified by the Barents Sea, *Mar. Geol.*, 85(2–4), 251–272, doi:10.1016/0025-3227(89)90156-4,  
440 1989.

441 Willeit, M., Ganopolski, A., Calov, R. and Brovkin, V.: Mid-Pleistocene transition in glacial cycles explained by  
442 declining CO<sub>2</sub> and regolith removal, *Sci. Adv.*, 5, eaav7337, doi:10.1126/sciadv.aav7337, 2019.

443